PPPL-2013

UC20-F

I-10362

PPPL-2013

DR-1609-8

PLASMA ROTATION IN THE POX TOKAMAK

By

K. Brau, M. Bitter, R.J. Goldston,
D. Manos, K. McGuire, and S. Suckewer

JUNE 1983

PLASMA
PHYSICS
LABORATORY

PRINCETON UNIVERSITY
PRINCETON, NEW JERSEY

PREPARED FOR THE U.S. DEPARTMENT OF ENERGY,
UNDER CONTRACT DE-AC02-76-CHO-3073.

DISCLAIMER

PLASMA ROTATION IN THE PDX TOKAMAK

K. Brau,* M. Bitter, R. J. Goldston, D. Manos, K. McGuire,

and S. Suckewer

Plasma Physics Laboratory, Princeton University,

Princeton, New Jersey 08544

ABSTRACT

Toroidal and poloidal rotation has been measured in the Poloidal Divertor Experiment (PDX) tokamak in ohmic-and neutral-beam-heated plasmas in a variety of discharge conditions and in both circular and diverted configurations. Rotation velocities were deduced from Doppler shifts of magnetic dipole (M1) lines and lines of optically allowed transitions in the visible and UV regions, from K_α emission, and also from an array of magnetic pickup loops. Poloidal and toroidal rotation velocities in ohmically heated discharges were usually less than 3×10^5 cm/sec. Near the plasma edge the toroidal rotation velocity varies with poloidal angle both before and during neutral-beam injection. No systematic poloidal rotation was observed during neutral-beam injection centered about or displaced 10 cm from the horizontal midplane, which implies that the poloidal damping time $\tau_\theta < 0.5\tau_{ii}$, consistent with theoretical estimates. The central toroidal rotation velocity during neutral-beam injection scales linearly with the quantity $P_{abs}/\overline{n_e}$ and is independent of plasma current and toroidal magnetic field. The toroidal rotation velocity is higher in deuterium than in hydrogen plasmas, and also in diverted as compared with circular discharges. Toroidal rotation decay times after injection range from 80-100 msec at the center to 160-180 msec at half the minor radius. Modeling of the radial profile of toroidal rotation indicates a central momentum diffusivity on the order of $8 \times 10^3 cm^2/sec$. This is approximately a factor of three higher than the momentum diffusivity obtained from the decay time. All present theories are inadequate in accounting for the observed damping rate of v_φ.

---

* Current address: Association Euratom-CEA sur la fusion,
Departement de recherches sur la fusion controlee,
Centre d'etudes nucleaires,
Fontenay aux Roses, France

INTRODUCTION

Interest in the subject of plasma rotation has grown in recent years as a result of the increased use of neutral beam injection systems on tokamaks. The large toroidally unbalanced forces associated with neutral beam injection are capable of inducing plasma flows which approach a modest fraction of the hydrogen ion thermal velocity. In this regime where the standard neoclassical assumption about the ordering of the plasma flow in powers of $v_{\parallel}/v_{th}$ breaks down, Kelvin-Helmholtz instabilities can also be driven. Furthermore, if the rotation velocity of the impurity ions is comparable to their thermal velocity, a situation which may occur in present tokamaks for some high Z impurities, the radial transport of ions can be modified. There have been a number of recent theoretical efforts devoted to theoretical[1-3] and experimental[4-6] investigations of radial impurity transport during co- and counter- neutral beam injection. Another effect which may be related to large toroidal rotation is the appearance of poloidal asymmetries in the electron density distribution during neutral beam injection.[7] Finally, it is possible that measurements of the rotation damping rate, which in previous experiments as well as our own has been shown to be nonclassical,[8] may provide insight into the role of magnetic or electrostatic fluctuations in ion radial transport.[9,10]

Poloidal flow velocities in tokamaks with toroidally unbalanced neutral beam injection are in our measurements many times lower than the toroidal velocities, even in cases where the poloidal and toroidal forces on the plasma are comparable. This is a result of the strong damping of poloidal flows by magnetic pumping, a process which converts the translational energy of a plasma

moving across a spatially varying magnetic field into thermal energy without radial transport. Poloidal rotation damping times are on the order of or less than an ion-ion collision time,[11-13] and are therefore much shorter than the toroidal damping times.

The PDX tokamak is very well-suited to the investigation of plasma rotation because of its flexibility in producing different discharge configurations and its full complement of diagnostics. Three of these diagnostic systems, a rapid scanning mirror and monochromator, an X-ray curved crystal spectrometer, and an array of magnetic pickup loops, provide a mutually supporting set of measurements of toroidal and poloidal rotation.

This paper is divided into four sections. First, the diagnostic systems employed in the measurement of toroidal and poloidal rotation are described. In Sec. II the experimental results are presented and compared with the PLT measurements of toroidal rotation. In Sec. III the toroidal rotation profile and its time evolution are modeled by a numerical simulation in order to determine the plasma viscosity profile. Finally, experimental results are compared with theoretical predictions of the poloidal and toroidal rotation damping in Sec. IV.

I. EXPERIMENTAL TECHNIQUES

The three diagnostics employed in the measurement of rotation are indicated in Fig. 1. The upper figure is a schematic of the PDX Fast Rotating Mirror (FARM) system. Poloidal and toroidal rotation velocities are measured from the Doppler shift of ion spectral line radiation. Instead of using the

previously described technique of simultaneous spatial and spectral scans,[8] the position of the four-sided mirror is set to a predetermined line of sight during the entire discharge with continuous spectral scanning. To determine the location of maximum line emissivity, radial and/or toroidal scans (without accompanying spectral scans) are performed of chosen ion lines. Doppler shifts are measured by comparing spectral profiles of impurity lines viewing along chords which are parallel and antiparallel to the direction of rotation. An advantage of this method is that it provides a continuous monitoring of the Doppler shift every 5 msec rather than approximately every 50 msec, as obtained with the earlier method. In addition, it can be employed when the impurity signals are short-lived, as, for example, occurs during impurity injection. A second difference with the earlier method of measuring Doppler shifts is that the angular deflection of the vibrating mirror is read out at two points during its sweep. The Doppler shift of a spectral profile is determined in reference to this fixed angular position rather than to the adjacent profile. The advantage of this procedure is that the Doppler shift can be determined even if only one spectral profile is available.

Near the center of the discharge, long wavelength magnetic dipole ("forbidden") transitions in the ground configuration of highly ionized medium and high Z elements such as titanium, scandium, and chromium were used. In plasmas contaminated by titanium impurities, one or two of the magnetic dipole lines of titanium, the dominant metallic contaminant in the plasma, were observable using only intrinsic levels of the impurity. In general, the most intense signals were obtained using the technique of impurity injection by laser blow-off. By selecting the elements to be injected and choosing wavelengths to

monitor different ionization states, the plasma rotation was measured at several minor radii. An advantage of impurity injection is that the resulting signal is easily distinguished from background radiation because of its characteristic time dependence. However, because the signals may persist for only 10-30 msec after the time of injection, the number of Doppler shifts that can be measured in a single discharge is small. It is desirable to obtain as many spectral profiles as possible because the uncertainty in the measurement of the flow velocity is reduced by averaging over individual Doppler shifts. In all of the subsequent measurements of rotation the quoted error is a combination of the uncertainty of a single Doppler measurement, usually 5×10^5 to 1×10^6 cm/sec depending on the intensity of the line, and the number of shifts which are averaged. Thus the experimental uncertainty in the determination of the flow velocity ranges from a minimum $\pm 2 - 3 \times 10^5$ cm/sec for C V lines to approximately $\pm 6 \times 10^5$ cm/sec for most of the impurity injection data.

The Bragg X-ray crystal spectrometer is shown in the middle of Fig. 1. This is primarily an ion temperature diagnostic which measures the Doppler broadening of the 2.61 Å K_α resonant line of Ti XXI.[14] Virtually all of the emission arises within the central 5 cm of the plasma because Ti XXI is the most abundant ionization state in the center of the discharge for $T_e(0) > 800$eV and also because the excitation rate of the K_α transition is a rapidly increasing function of electron temperature. The angle between the line of sight and the radial direction on the magnetic axis is 16°, so that a fraction ($\sin 16° = 0.28$) of the toroidal rotation velocity can be observed from the Doppler shifts of the K_α line. Spectra are recorded during 16 con-

secutive time intervals of 25 msec of each discharge. To reduce the statistical error, data are usually accumulated from several discharges with similar parameters. The absolute value of the Doppler shift is determined by comparing the centroids of the spectral profiles during neutral beam injection with those either before or long after injection. Under normal circumstances the drift in the position of the energy channel corresponding to the centroid of the K_α transition with no Doppler shift is less than one channel over the course of an operating day. The uncertainty in v_φ is approximately $\pm 3 \times 10^6$ cm/sec.

The third diagnostic is a poloidal array of magnetic pickup loops, also called Mirnov coils, (bottom of Fig. 1) which detect rotating MHD structures in the plasma. The direction of rotation is determined by comparing the phase of oscillation between adjacent pickup loops (see Fig. 1). The rotation phase velocity can be determined from these signals as a function of the plasma radius if the radial location and mode structure of the MHD instability are known. From this the plasma rotation can be inferred. The MHD characteristics are measured using a soft X-ray surface barrier diode array. One problem with this technique is that it is impossible to distinguish between poloidal and toroidal rotation. A second difficulty is that the rotation of the MHD instability may not be connected with the translation of the bulk plasma. For example, in the case of the recently discovered MHD activity, dubbed "fishbone" oscillations,[15] which are caused by an internal m=1 kink instability, the mode appears to be associated with the toroidal precession velocity of the injected high energy beam ions rather than with the rotation of the bulk plasma. This velocity can be a factor of five larger than the local bulk ion rotation velocity. Under certain

conditions mode oscillations can be identified with the toroidal translation of the bulk plasma. The toroidal velocities deduced from the $\dot{B}_\theta$ loops represent a lower bound on the rotation velocity since there is usually an additional poloidal mode rotation in the electron diamagnetic direction opposite to the toroidal velocity. Due to this effect, these measurements may be in error by as much as 15%. The radial position of the mode resonant surface determined from the soft X-ray measurements is known to within ± 2 cm.

II. EXPERIMENTAL RESULTS

A. Ohmically heated plasmas

Toroidal and poloidal rotation in ohmically heated plasmas were investigated by the FARM diagnostic. Central and near central rotation were measured by the Doppler shift of a titanium magnetic dipole line (Ti XVII 3834 Å) and edge rotation was measured using a carbon line in second order (C V 2271 Å). Both of these elements are present in the plasma as intrinsic impurities. For all of the measurements, Doppler shifts were averaged during the steady-state portion of discharge to reduce the experimental error. For these discharges $I_p = 300 - 500$ kA, $B_T \sim 21$ kG, and $\overline{n_e} \sim 2 - 3 \times 10^{13}\text{cm}^{-3}$. Within the experimental uncertainty (3×10^5 cm/sec) no poloidal rotation was observed, either near the center or the edge of the plasma. The toroidal rotation velocity of C V at the edge of the plasma ($r/a \sim 0.9$), which was deduced from measurements along the two lines of sight tangent to the

inner major radius side of the emitting shell, was also zero within the error bars. (In a later section of this paper it will be shown that the toroidal velocity of C V along the *outer* major radius side of the shell is $\sim 4 \times 10^5$ cm/sec in the direction opposite the current.) The near central ($r \sim 5-10$ cm) toroidal rotation as observed from a set of approximately ten ohmically heated discharges, was less than 3×10^5 cm/sec, except for three of the discharges for which the toroidal rotation velocity was approximately 1×10^6 cm/sec. The parameters for these discharges were as follows: $B_T = 12$ kG, $T_e(0) \sim 700-800$ eV, $I_p \sim 270$ kA, and $\overline{n_e} \sim 2.5 \times 10^{13} \mathrm{cm}^{-3}$. There was relatively little variation in the electron density or temperature profiles, or in the MHD activity or soft X-ray emission among the discharges with $v_\varphi \sim 10^6$ cm/sec compared to those in which $v_\varphi < 3 \times 10^5$ cm/sec.

Based on measurements of the mid-central ($r \sim 20-25$ cm) toroidal rotation in ohmically heated plasmas in different sets of discharge conditions ($B_T = 21$ kG, $T_e(0) \sim 1.4$ keV), no rotation was observed when the data were averaged over time intervals of 100 msec. However, on a short (< 10 msec) time scale the toroidal velocity seemed to fluctuate about a mean value of zero as shown in Fig. 2. This represents two successive spectral scans of Ti XVII 3834 Å from the same discharge and separated in time by approximately 10 msec. The distance between the first and third peaks, equal to the spectral scan period, must be constant in time unless the Doppler shift is changing rapidly on this time scale. (Based on spectral scans of an Hg line from a pen lamp during a PDX discharge, the vibration period of the scanning mirror is constant to within 0.1 %, approximately one tenth of the shift indi-

cated in the figure.) The displacement between the spectral peaks in the two cases (dashed and solid lines) is well beyond the error bars, and corresponds to a Doppler shift velocity of about 1.6×10^6 cm/sec. As a quantitative measure of the magnitude of the velocity fluctuations, the quantity $(\langle \Delta v \rangle^2)^{1/2}$ in ohmically heated discharges has been determined from several hundred Doppler shift measurements. For Ti XVII and C V, $(\langle \Delta v \rangle^2)^{1/2} \simeq 9 \times 10^5$ cm/sec and 3×10^5 cm/sec, respectively. The width of the fluctuation spectrum of Ti XVII is a factor of three larger than the experimental uncertainty.

B. Poloidal rotation with neutral beam injection

As alluded to earlier in this paper, poloidal rotation velocities induced by neutral beam injection are several times smaller than toroidal rotation (for toroidally unbalanced momentum input) because of the strong parallel viscous damping associated with flows transverse to a spatially varying magnetic field. Poloidal rotation is thus difficult to detect experimentally; to our knowledge there have been no published measurements to date on poloidal rotation during neutral beam injection. In our experiments we have attempted to determine typical poloidal rotation velocities induced by neutral beam injection, and to establish an upper limit on the rotation damping time. While it may appear that for neutral beam injection centered about the magnetic axis no net poloidal momentum is imparted to the plasma, in PDX there are two ways of obtaining substantial momentum input in the poloidal direction. The first is to inject the beams above or below the magnetic axis. In PDX the vertical coordinate of the magnetic axis can be varied as much as 10 cm in either direction using a

combination of movable rail limiters and a magnetic feedback network. Since the radius of the injected neutral beam is about 8 cm, it is possible to inject all of the momentum from the neutral beam either above or below the magnetic axis. A second source of poloidal momentum present in standard $z_m = 0$ or vertically uncentered $z_m = \pm 10$ discharges, where z_m is the vertical coordinate of the magnetic axis with respect to the PDX horizontal midplane, arises from the radial current of the beam ions. This process will be described in a later section of this paper. The FARM diagnostic was used to investigate poloidal rotation during neutral beam injection into vertically centered ($z_m = 0$) and uncentered ($z_m = \pm 10$ cm) discharges.

In Fig. 3 poloidal plasma rotation at the edge ($r/a \sim 0.85$, $z_m = 0$) measured from the C V line and averaged in 50-100 msec intervals is plotted as a function of time for a $D^0 \rightarrow H^+$ circular discharge. According to the figure, the poloidal rotation appears to be less than 2×10^5 cm/sec. Measurements of the near central poloidal rotation ($r/a \sim 0.5$, $z_m = 0$) during neutral beam injection (3.5 MW $D^0 \rightarrow H^+$) deduced from Doppler shifts of Ti XVII using intrinsic levels of titanium impurity are plotted in Fig. 4. Each point represents an average of 2-10 Doppler shifts obtained in a 50 to 100 msec interval for a single discharge. The large scatter of the data about the mean value of zero indicates that the poloidal rotation is zero to within $\pm 3 \times 10^5$ cm/sec. This result was also obtained during subsequent measurements of the poloidal rotation of Ti XVII using impurity injection. In a preliminary report poloidal rotation speeds on the order of 1.5×10^6cm/sec during neutral beam injection were quoted.[16] These preliminary results, however, were based on a very small set

of data. After more careful analysis, we believe that these measurements were affected by a source of gamma ray noise and led to erroneous results. From the data available now we conclude that in the region $a/2 < r < a$ the poloidal rotation is less than 3×10^5 cm/sec.

In another series of experiments an attempt was made to induce poloidal rotation by injection into vertically uncentered ($z_m = \pm 10$ cm) discharges. Poloidal rotation was measured from the Doppler shift of Sc XVI 4530 Å at $r \sim 25$ cm. In the case of a plasma raised 10 cm, there was perhaps a slight poloidal rotation in the direction expected from the momentum input. However, the amount of rotation ($\sim 2 \times 10^5$ cm/sec) was smaller than the experimental uncertainty ($\sim 6 \times 10^5$ cm/sec). Measurements of v_θ in plasmas with $z_m = -10$ cm also indicated no poloidal rotation, although the size of the data set was smaller. (The possibility of observing poloidal rotation with off axis injection could be increased by measuring the Doppler shift of impurities located at r=10 cm, the position of maximum momentum input from the beams. Unfortunately, the magnetic dipole line emission from higher ionization states of scandium located closer to the center of the discharge was too weak to perform these measurements.) We again conclude that poloidal rotation velocities in the region $a/2 < r < a$ in PDX are smaller than the experimental limit of detection. In a later section of this paper we shall use these results to calculate an upper limit for the poloidal rotation damping time.

C. Toroidal rotation with neutral beam injection

The goals of the toroidal rotation studies in neutral beam heated plasmas were to investigate the scaling of the toroidal rotation velocity with different neutral beam and plasma parameters, and to measure the radial profile of the toroidal rotation and its rate of decay after injection. From these results it may be possible to derive general arguments about the relationship between momentum and energy confinement. In Fig. 5 we have plotted the maximum central rotation velocity in circular $D^0 \rightarrow H^+$ discharges as a function of $P_{abs}/\overline{n_e}$, where P_{abs} is the absorbed beam power and $\overline{n_e}$ the line averaged electron density. The injection energy of the beam particles is approximately 50 keV. Each of the 16 points in the figure represents a set of 5-20 discharges with nearly identical discharge conditions.

From Fig. 5 it appears that toroidal rotation scales linearly with $P_{abs}/\overline{n_e}$. (In PDX the ion temperature obeys a similar scaling at fixed B_T and I_p.) If the same 16 values of v_φ are plotted as a function only of P_{abs} (not shown), it is found that the toroidal rotation tends to saturate at highest injection powers where the electron densities are also the highest. By contrast, in PLT the central rotation speed appeared to be independent of the electron density and linearly dependent on beam power.[17] Thus, the PLT data pointed to an increase in momentum confinement with increasing n_e and no dependence on P_b. In PDX the linear dependence of v_φ on $P_{abs}/\overline{n_e}$ implies that the momentum confinement time is independent of n_e. This inference is based on the assumption that there are no unknown parameters associated with the high density and high beam power discharges, which may be responsible for the observed saturation

of v_φ. The data also appear to indicate that v_φ is independent of I_p. This result is in contrast to the marked dependence of ion thermal confinement or bulk energy confinement on I_p in PDX. It should be emphasized that these data were acquired over a period of months and that there are no data available from single parameter "current scans," i.e., sets of discharges from a limited period of operation in which all parameters were kept constant while the current was varied. This might have revealed more conclusively the dependence (or lack thereof) of v_φ on I_p.

The dashed line fit to the data is essentially a measure of the amount of toroidal momentum input from the neutral beams which is stored in the plasma. To compare this with the PLT result we must correct for the difference in the direction of neutral beam injection. When this correction is accounted for, the central toroidal rotation speed in PDX is nearly a factor of two larger than in PLT for the same beam momentum input, at a density of $3 \times 10^{13}\text{cm}^{-3}$ in PLT. There are, however, cases in PLT where the ratio of v_φ to input torque is only $\sim 30\%$ less than that of PDX. Because of the difference in the scaling of toroidal rotation in PDX and PLT with respect to electron density, the ratio of the viscosities of the two tokamaks depends on electron density. We have at present no satisfactory explanation of why the effective viscosity in PDX is much lower than in PLT; however, it will later be shown that a comparison of the toroidal rotation damping rates leads to a qualitatively similar conclusion.

In Fig. 6 we have plotted v_φ vs. $P_{abs}/\overline{n_e}$ for a set of neutral beam heated deuterium discharges. If the relative rotation velocities were given by the ratio of momentum input to plasma mass, all of the points would lie beneath

the dashed curve. The point corresponding to $D^0 \rightarrow D^+$ is less than the velocity for $D^0 \rightarrow H^+$, but is still larger than the ratio of the plasma masses. Hence, we conclude that the momentum confinement time is longer for deuterium than hydrogen discharges, as observed in PLT. The discrepancy between the observed v_φ and that predicted on the basis of the beam to plasma ion mass ratio is even larger for the case of H^0 injection. A possible explanation for this discrepancy is the following: the hydrogen injection measurements were all obtained in diverted discharges in which the plasma boundary is defined by a magnetic separatrix rather than a set of rail limiters. The rotation velocity in diverted discharges may not be constrained to vanish at the edge of the diverted plasma in the same way as a limiter plasma, and the total damping rate may therefore be lower in diverted discharges.

The momentum confinement time can also be determined from the decay of rotation after neutral beam injection. Figure 7 is a plot of the time evolution of the toroidal rotation at r=0 and r=25 cm during and after neutral beam injection for a set of relatively high current (I_p = 480 kA), relatively high field (B_T =21.7 kG), moderate density ($\overline{n_e} = 2.9 \times 10^{13}\text{cm}^{-3}$), circular discharges with 3.5 MW $D^0 \rightarrow H^+$. (These data are used later in the modeling of the perpendicular viscosity.) In Figs. 8(a) and (b) the $1/e$ decay times τ_φ of the central toroidal rotation have been plotted as functions of $\overline{n_e}$ and I_p for $D^0 \rightarrow H^+$ circular discharges. For roughly half the data, the toroidal rotation was observed to decrease between 25 and 50 msec before the end of the beam pulse. These cases are not included in Fig. 7. There appears to be no dependence of τ_φ on I_p or $\overline{n_e}$. In general, τ_φ lies within the range 80-100 msec. Based

on measurements of the Doppler shift of Ti XVII in four sets of $D^0 \rightarrow H^+$ circular discharges with injection powers ranging from 3.0 MW to 5.5 MW at $r = 20-25$ cm, τ_φ varies from 160 to 180 msec (see Fig. 7). The central toroidal decay times are approximately a factor of two to four longer in PDX than in PLT. When the beam stopping time ($\sim$ 15 msec) after neutral beam injection is subtracted from the $1/e$ decay times, the difference between the PDX and PLT results is somewhat larger. This result is not quantitatively consistent with the observation of central rotation velocities which are at most a factor of two higher in PDX than in PLT for the same toroidal momentum input, although both results indicate that the momentum confinement is greater in PDX.

Figure 9(a) is a plot of v_φ versus minor radius for the same set of discharges plotted in Fig. 7. This figure includes measurements by all three of the rotation diagnostics: at r=0 (Ti XXI K_α), r=12 cm ($\dot{B}_\theta$ loops), and r=25 and 38 cm (Ti XVII and C V). The half-width of the profile is about 22 cm, which is comparable to the width of the toroidal rotation profile in PLT. Figure 9(b) is a plot of the toroidal rotation profile for a set of moderately low TF (B_T=15 kG), high density ($\overline{n_e} = 4.8 \times 10^{13}\text{cm}^{-3}$), 3.1 MW $D^0 \rightarrow H^+$ circular discharges. The majority of the measurements were obtained using laser blow-off injection of scandium and titanium and all were made slightly before the end of the beam pulse. There are no data on the decay of toroidal rotation after neutral injection for these discharges.

The remaining measurements of v_φ with neutral beam injection were obtained over a period of several months of low field operation (B_T = 8 – 15 kG) during circular $D^0 \rightarrow H^+$ discharges. In Fig. 10 the quantity

$v_\varphi(r)\overline{n_e}/P_{abs}$ has been plotted as a function of minor radius for co- and counter-injection. Also shown is the toroidal rotation profile plotted in Fig. 9(a) divided by the quantity $P_{abs}/\overline{n_e}$. In the small number of cases where the quality of radial scans of impurity emission was too poor to obtain the emissivity profile, the position of the maximum intensity was deduced from the electron temperature profile and previous radial scans of the impurity. The uncertainty in the radial position of these points (which include both of the counter-injection results) may be as high as ± 4 cm. The overlap between the normalized toroidal rotation profiles for the high and low toroidal field data suggests that v_φ is independent of toroidal field. Again it should be noted that the plasma conditions for these discharges varied over a wide range and that the independence of v_φ on B_T is not firmly established.

In the data presented above it has been assumed that the toroidal velocity is constant on a flux surface. We now present evidence which indicates that this assumption may not be valid near the edge of the plasma. Figure 11 is a plot of the toroidal rotation velocity of C V before and during neutral beam injection ($D^0 \rightarrow H^+$) in a set of circular discharges along three different lines of sight. The upper curve is a measurement of v_φ along two chords tangent to the C V shell on the small major radius side of the discharge, while the lower curve was obtained on the outboard side. Each point represents an average of 50-200 individual Doppler shifts. Along the horizontally scanning lines of sight which are tangent to the inboard side, there is a small contribution to the total signal intensity arising from the outer shell. In general, the Doppler shift of C V measured from these two emitting regions will not be the same because

of the different angles between the sight line and the direction of rotation. We have found that this reduces the actual Doppler shift by approximately ten percent. On the outboard side of the flux surface before neutral beam injection the toroidal rotation velocity of C V is 4×10^5 cm/sec in the direction opposite the plasma current, and zero on the inboard side. While this result is somewhat surprising, the difference in toroidal velocity during the ohmically heated phase of the discharge is comparable to the poloidal variation in v_φ predicted from neoclassical theory.[18] (This variation arises due to the condition of divergence-free flow and the fact that the toroidal field is a function of poloidal angle.) During neutral beam injection an additional toroidal translation at 5×10^5 cm/sec was imparted equally to the entire flux surface. Because the neutral beam induced rotation is divergence-free, the poloidal variation in v_φ should remain the same.

III. TOROIDAL ROTATION MODELING

The reader is referred to a previous paper[17] for a description of the numerical code which simulates momentum deposition during neutral beam injection and which is used to determine the viscosity profile $\chi(r)$. The temporal and spatial evolution of the toroidal rotation velocity is assumed to obey a diffusion equation of the form

$$m\frac{\partial}{\partial t}nv_\varphi = \mathbf{F}_\varphi(r,t) - \frac{1}{r}\frac{\partial}{\partial r}rnm\chi(r)\frac{\partial v_\varphi}{\partial r} - \frac{nmv_\varphi}{\tau_{CX}} \qquad (1)$$

where $\mathbf{F}_\varphi(r,t)$ is the input force from the beams in the toroidal direction, and

$$\tau_{CX}{}^{-1} = n_0\langle\sigma v\rangle\frac{T_i}{T_i - T_0} \qquad (2)$$

is the damping due to charge exchange, where T_i and T_0 are the temperatures of the ionic and neutral species, respectively. The relative velocity $v = v_{\varphi 0} - v_{\varphi i}$ has been approximated in this formula by using the relation

$$\frac{v_{\varphi 0}}{v_{\varphi i}} \simeq \frac{T_0}{T_i}. \tag{3}$$

Most of the uncertainty in τ_{CX} relates to the determination of the neutral density profile. The value of n_0 is deduced to roughly a factor of three accuracy from measurements of the neutral flux by a charge exchange analyzer. A one-dimensional neutral particle transport code is used to calculate both $n_0(r)$ and $T_0(r)$.

To calculate $\mathbf{F}_\varphi(r)$ the deposition code follows the trajectories of a test sample of 3000 neutral beam particles from the time of their initial ionization in the plasma until the time they are lost from the discharge or slow down to the local thermal energy. A Fokker Planck collision operator is used to calculate the momentum transferred between beam ions and the various plasma species via drag, pitch angle scattering, and energy diffusion. These collisions are calculated in the frame of reference of the rotating plasma. When beam ions slow down to $3T_i/2$ in the plasma frame, they are considered to be thermalized, and provide a small "thermalization force." We assume that this thermalization force roughly balances the $m_i v_\varphi \partial n/\partial t$ term on the left-hand side of Eq. (1), and so we neglect it. A more complete treatment would include fully time-dependent density profiles, as well as an additional convective term in Eq. (1). We estimate that these effects are relatively small for our present conditions. There is an additional force on the plasma which arises from the radially-inward motion of co-injected beam ions. This radial beam current drives a radial electric field,

which is damped by a radial plasma current, in the usual model of this process. This plasma current absorbs the beam momentum through the $\mathbf{j}_r \times \mathbf{B}_p$ force. In the case of perpendicular injection, this process can account for 10–20 % of the total torque on the plasma.

The viscosity profiles $\chi(r)$ which produce the best fit to the toroidal rotation profile shown in Fig. 9(*a*) are plotted in Fig. 12(*a*). To determine the sensitivity of χ at the edge to the charge exchange damping rate, the neutral density and flow velocity were varied. In all cases the toroidal flow velocity is assumed to vanish at the limiter boundary. Curve *a* is the standard case; in curve *b* the neutral density was increased by a factor of three; in curve *c* the neutral flow velocity was taken to be zero. As expected, uncertainties in the edge neutral density and/or flow velocity affect primarily the calculation of the edge viscosity. Figure 12(*b*) is a plot of the same three curves for the toroidal rotation profile in Fig. 9(*b*). Because of the higher electron density and smaller fraction of neutral particles, charge exchange damping in all three cases is relatively unimportant. In this case edge rotation is damped by collisions between the plasma ions and the wall rather than with neutral particles.

When the standard viscosity profile for the first data set is used in the time dependent momentum diffusion equation, the calculated momentum damping times are 25 msec, about a factor of three shorter than observed. In fact no viscosity profile is capable of reproducing both the shape of the rotation profile and decay times with the momentum deposition profile calculated by the simulation. If $\chi(r)$ is reduced in order to produce agreement with the observed decay time, the central rotation speed is a factor of two to three larger than the

experimental value. Both the radial profile and time evolution of the rotation can be reproduced by a single viscosity profile if the momentum deposition profile was somewhat narrower and lower in magnitude by a factor of two to three. However, because total momentum is conserved, any reduction in the collisional force profile must be balanced by an increase in the momentum lost from the plasma, via charge exchange, orbit losses, or shine through. For example, in the case corresponding to Fig. 11(a) approximately 70% of the input momentum is absorbed by the plasma while the remaining 30% is lost to the vacuum vessel. In order to obtain a momentum deposition profile leading to a time independent value of $\chi(r)$ these percentages would have to be reversed. If the $\mathbf{J} \times \mathbf{B}$ force were, for some reason, ineffective, the results would still not be consistent with experiment.

It is possible that the momentum confinement time in PDX is smaller during neutral beam injection than during the ohmic phase of the discharge. This hypothesis is supported by the fact that the ratio of equilibrium rotation velocities at fixed $\overline{n_e}$ and momentum input in PDX and PLT ($\lesssim 2$) is less than the ratio of the $1/e$ decay times of the rotation ($\sim 2-4$). In PLT a single viscosity profile $\chi(r)$ was found to model both the toroidal rotation profile and the decay rate. The two preceding statements taken together imply that $\chi(r)$ may depend on the presence or absence of neutral beam injection in PDX. Furthermore, in these PDX discharges the energy confinement time is a factor of two to three lower during neutral injection than during OH plasmas[19] and increases to its pre-injection value within ~ 20 msec based on magnetic equilibrium measurements. To confirm this hypothesis, however, the connection between the energy and

momentum confinement time must be demonstrated.

IV. COMPARISON OF ROTATION DAMPING TIMES WITH THEORY

A. Ohmically heated plasmas

In this section we compare the experimentally observed toroidal flow velocities with the predictions of neoclassical transport theory. In ohmically heated plasmas the parallel flow velocity of the ions is given by the expression

$$v_{\parallel} = -\frac{cT_i}{eB_\theta}\left[\frac{n_i'}{n_i} + \frac{e\phi'}{T_i} + k\frac{T_i'}{T_i}\right] \tag{4}$$

where $k = -.17, 1.5$, or 2.7 for ions in the collisionless, plateau, or collisional regimes.[20 22] The introduction of trace impurities into the plasma does not alter the above expression provided the contribution of the impurity viscosity to the total ion viscosity is small [22] In PDX where plasmas are relatively clean ($Z_{eff} < 2$) this condition is usually satisfied. Hence, by measuring the toroidal velocity of the impurity ions and the radial profiles of the ion temperature and density, it is in principle possible to deduce the local value of the electric field. Near the center of the plasma where n_i and T_i are relatively flat, the calculation of E_r may vary by a factor of three depending on the value chosen for the density and temperature gradients. Using the plateau regime formula for $v_{\parallel}$ and taking $v_{\parallel} \sim 1 \times 10^6$ cm/sec, we have $E_r \sim -10$ to $+5$ V/cm. At $r \sim 20$ cm, where the uncertainties in T_i' and n_i' are lower, we find, taking $v_{\parallel} \sim 0$, $E_r \sim 100$ V/cm.

B. Poloidal rotation damping

Three authors[11-13] have obtained different expressions for the damping rate of poloidal rotation in a toroidally confined plasma in the plateau-collisionless regime, viz.

$$\tau_\theta \sim \tau_i \left(\frac{r}{R}\right)^\alpha \tag{5}$$

where α=0, 1, or 1.5. To estimate an upper bound for τ_θ from the experimental data, we may use both the results of the experiments with on- or off-axis neutral beam injection. For off-axis injection it is relatively simple to calculate the momentum absorbed by the plasma in the poloidal direction and thus to estimate τ_θ by balancing the input force against the poloidal viscosity. (The $\mathbf{j} \times \mathbf{B}$ force, which is also present, is approximately a third as large as the direct collisional force from the beams, and has been neglected.) Taking $v_\theta < 5 \times 10^5$ cm/sec at $r = 25$ cm, we obtain $\tau_\theta \lesssim \tau_{ii}$. In the case of on-axis injection there is a net force in the poloidal direction due to the $\mathbf{j} \times \mathbf{B}$ reaction force of the plasma induced by the radial current of the injected beam ions. This force is larger in the poloidal than in the toroidal direction by a factor B_T/B_p. Based on a value for the $\mathbf{j} \times \mathbf{B}$ force obtained in the numerical simulation of the momentum deposition, and taking $v_\theta < 3 \times 10^5$ cm/sec at r=25 cm for 4.5 MW $D^0 \rightarrow H^+$ injection, we find $\tau_\theta < 0.5\tau_i$. Hence, within the accuracy of the experimental data, α may be equal to any of the values quoted above.

C. Toroidal rotation damping

Early theoretical calculations of the perpendicular ion viscosity were

based on the assumption that the parallel flow velocity of the ions was much less than the thermal velocity. In tokamaks with toroidally unbalanced neutral injection, such as PDX, this assumption breaks down for the impurity ions. Some theoretical effort has lately been devoted to the problem of perpendicular ion viscosity in the high flow velocity regime. In the following discussion of the PDX results in relation to these calculations of χ in the high flow velocity regime, it should be emphasized that the theoretical results are not yet firmly established.

The calculation of the perpendicular viscosity in a collisional plasma[23] is based on a solution of the Braginskii fluid equations[24] and uses a multiple time scale approach to determine the conductivity tensor. The viscosity is approximately given by

$$\chi = \eta(1 + 2.3q^2) \tag{6}$$

where $\eta = 6T_i/5m_i\Omega^2\tau_i$ is the classical perpendicular fluid viscosity. The neoclassical perpendicular viscosity is therefore related to the classical viscosity in a manner similar to the relationship between neoclassical and classical ion heat conduction. Although the calculation is strictly valid only for the collisional regime, it has been suggested that the neoclassical ion viscosity scales in the same way as the heat conduction in the transition from the fluid to the collisionless regimes; i.e., $\chi(r) \sim \rho_i^2 q^2 \nu_i \epsilon^{-3/2}$.[23] In PDX the main ions in neutral beam heated plasmas on axis are in the plateau regime. Substituting PDX parameters for the first toroidal rotation profile, we obtain for the neoclassical viscosity $\chi_{neo}(r) =$ 60cm^2/sec at r=0, 500cm^2/sec at r=25 cm, and 1.5×10^3cm^2/sec at r=44 cm. The discrepancy between χ_{neo} and χ_{exp} varies between a factor of 10 to 50 at the edge to a factor of 100 at the center. This implies no agreement with the

neoclassical fluid model of perpendicular viscosity.

Another approach to the determination of χ_{neo} in the high flow velocity regime[25] is based on the drift kinetic equation. The expressions for the perpendicular ion viscosity in the different collisionality regimes are identical with expressions obtained previously[20] with the assumption of low flow velocity. For the case of collisionless plasmas

$$\chi = \frac{1}{10} q^2 \rho^2 \nu_i. \tag{7}$$

Substituting PDX parameters for $r \sim 0$, we have $\chi = 3\text{cm}^2/\text{sec}$, which is more than three orders of magnitude lower than the empirically determined value. Thus present neoclassical theories of toroidal rotation damping show no agreement with present PDX tokamak results, implying that the theories are completely inadequate in explaining the observations.

The calculated central rotation damping time due to periodicity in the toroidal magnetic field (ripple) is greater than 5 seconds,[26,27] and thus cannot account for the observed decay of rotation. Two authors have recently considered the effect of magnetic and/or electric field perturbations on the damping of toroidal rotation.[9,10] If perturbed fields are spatially localized and not due to external field errors, then according to the theory, in the case of electrostatic perturbations, toroidal momentum is carried out at a rate comparable to the anomalous ion heat transport, i.e., $\kappa_i \sim \chi$. Based on an independent determination of the ion heat conductivity for the discharges used in the modeling of toroidal rotation, we have $\kappa_i \sim 1.5 \times 10^3\text{cm}^2/\text{sec}$. (This is equal to the neoclassical value[28] and is roughly 30% less than the ion loss due to convection

in this case.) This value of κ_i is approximately a factor of five less than the perpendicular viscosity. Again, the theory appears inadequate in accounting for the rotation damping.

SUMMARY

We have measured toroidal and poloidal rotation in the PDX tokamak from Doppler shifted impurity radiation in the visible, UV, and X-ray regimes, and from MHD oscillations. In ohmically heated plasmas the bulk poloidal and toroidal rotation velocities are less than 3×10^5 cm/sec, with the exception of near central toroidal flows, which can be on the order of 1×10^6 cm/sec. On a short (< 10 msec) time scale the toroidal flow velocity of Ti XVII at $r \sim 20$ cm appears to vary by as much as 10^6 cm/sec. At the edge of the plasma the toroidal rotation velocity of C V can be a function of poloidal angle. In neutral beam heated plasmas the poloidal rotation velocities are less than $3 - 6 \times 10^5$ cm/sec for the cases of off- and on-axis injection. These values imply that the rotation damping time $\tau_\theta < 0.5\tau_i$, which agrees with theoretical estimates.

Toroidal rotation induced by neutral injection scales linearly with $P_{\rm abs}/\overline{n_e}$, which is consistent with the notion that the momentum confinement time is independent of electron density. There is no clear dependence of beam induced toroidal rotation on either the plasma current or the toroidal magnetic field. Total momentum confinement is relatively higher in deuterium than in hydrogen plasmas, in diverted than in circular discharges, and in PDX than in

PLT. The decay times of the toroidal rotation after neutral beam injection range from 30-100 msec at the center to 160-180 msec at $r \sim 25$ cm. These are about a factor of two to four higher than in PLT for central rotation and more than a factor of four higher at $r \sim a/2$. Numerical modeling of the perpendicular viscosity indicates that the momentum confinement may be lower during neutral injection than during the ohmic phase of the discharge. There is as yet no adequate theoretical understanding of the mechanism(s) underlying toroidal rotation damping in PDX, and present neoclassical and anomalous models are completely inadequate in explaining the results.

ACKNOWLEDGMENTS

The authors would like to extend their thanks to J. T. Hogan, F. L. Hinton, R. D. Hazeltine, M. Kotschenreuther, R. E. Waltz, S. K. Wong, S. P. Hirshman, and M. N. Rosenbluth for helpful discussions on plasma rotation, to R. C. Isler for making certain data available prior to publication, and to R. Kaita and D. Buchenauer for providing some of the data presented in this paper. We are indebted to S. Cohen, and J. Timberlake for the operation of the impurity injection system, to H. Kugel for the smooth functioning of the neutral beams, and to K. Bol, H. Takahashi, M. Okabayashi, D. K. Owens, and M. G. Bell for the daily operation of PDX. A large engineering and technical crew must also be commended for their efforts: we wish to thank in particular D. Hay, G. Drozd, H. Feng, R. Mika, and G. D'Amico. This work supported by U. S. Department of Energy contract No. DE-AC02-76-CHO-3073.

REFERENCES

[1] STACEY, W. M., SIGMAR, D. J., Phys. Fluids, **22**, (1979) 2000.

[2] WONG., S. K., BURRELL, K. H., Phys. Fluids, **25**, (1982) 1863.

[3] PARKS, P. B., BURRELL, K. H., WONG, S. K., Nucl. Fusion **20**, (1980) 27.

[4] ISLER, R. C., MILORA, S. L., ARNURIUS, D. E., BATES, S. C., BURRELL, K. H., et al., in Plasma Physics and Controlled Nuclear Fusion Reasearch (Proc. 8th Int. Conf. Brussels, 1908) Vol. 1, IAEA, Vienna (1981) 53; also ISLER, R. C., CRUME, E. C., ARNURIUS, D. E., MURRAY, L. E., Impurity Transport During Neutral Beam Injection in the ISX-B Tokamak, Oak Ridge National Laboratory Report ORNL/TM-7472 (1980).

[5] ISLER, R. C., MURRAY, L. E., KASAI, S., ARNURIUS, D. E., BATES, S. C., et al., Phys. Rev. Lett. **47**, (1981) 649.

[6] SUCKEWER, S., COHEN, S., DAUGHNEY, C., DENNE, B., EFTHIMION, P., et al., Bull. Am. Phys. Soc. **27** No. 8, part II, (1982) 1044.

[7] REUSCH, M. F., OKABAYASHI, M., LARRABEE, D. A., JOHNSON, D., GREK, B., BRAU, K., SUCKEWER, S., Bull. Am. Phys. Soc. **27** No. 8, part II, (1982) 1048.

[8] SUCKEWER, S., EUBANK, H. P., GOLDSTON, R. J., HINNOV, E., SAUTHOFF, N., Phys. Rev. Lett. **43**, (1979) 207.

[9] WALTZ, R. E., Phys. Fluids, **25**, (1982) 1269.

[10] KOTSCHENREUTHER, M., Ph. D. thesis, Princeton Univ., (1982).

[11] STIX, T. H., Phys. Fluids, **18**, (1973) 1260.

[12] ROSENBLUTH, M. N., Bull. Am. Phys. Soc. **18**, series II, No. 10, (1973) 1337.

[13] HIRSHMAN, S., Nucl. Fusion **18**, (1978) 224.

[14] BITTER, M., VON GOELER, S., GOLDMAN, M., HILL, K. W., HORTON, R., et al., "Temperature, Its Measurement and Control in Science and Industry", ed. J. F. Schooley, American Institute of Physics, Vol. 5, (1982) 693.

[15] MCGUIRE, K., GOLDSTON, R., BELL, M., BITTER, M., BOL, K., et al., Phys. Rev. Lett. **50**, (1983) 891.

[16] SUCKEWER, S., BRAU, K., BITTER, M., COHEN, S., MANOS, D., et al., Bull. Am. Phys. Soc. **26** No. 7, (1981) 1000.

[17] SUCKEWER, S. EUBANK, H. P., GOLDSTON, R. J., MCENERNEY, J., SAUTHOFF, N. R., TOWNER, H. H., Nucl. Fusion **21**, (1981) 1301.

[18] HINTON, F. L., HAZELTINE, R. D., Reviews of Modern Physics, **48**, No. 2, Part I, (1976) 239.

[19] HAWRYLUK, R., ARUNASALAM, V., BELL, M., BITTER, M., BOL, K., et al. Phys. Rev. Lett. **49**, (1982) 1408.

[20] ROSENBLUTH, M. N., RUTHERFORD, P. H., TAYLOR, J. B., FRIE-

MAN, E. A., KOVRIZHNIKH, L. M., (1971), in Plasma Physics and Controlled Nuclear Fusion Research (proc. 4th Int. Conf. Madison, 1971) Vol. 1, IAEA, Vienna (1971) 495.

[21] HAZELTINE, R. D., Phys. Fluids, **17**, (1974) 961.

[22] HIRSHMAN S., SIGMAR, D. J., Nucl. Fusion, **21**, (1981) 1079.

[23] HOGAN, J., talk given at the Sherwood Theoretical Meeting, Oak Ridge Tennesee (1982).

[24] BRAGINSKII, S. I., Reviews of Plasma Physics, (LEONTOVICH, M. A., Ed.) Vol. 1, Consultants Bureau, New York (1965) 205.

[25] HINTON, F. L., WONG, S. K., Bull. Am. Phys. Soc. **27**, no. 8, part II, (1982) 1127.

[26] BOOZER, A. H., Phys. Fluids, **23**, (1980) 2283.

[27] BOOZER, A. H., Phys. Fluids, **19**, (1976) 149.

[28] CHANG, C. S., HINTON, F. L., Phys. Fluids, **25**, (1982) 1493.

FIGURE CAPTIONS

FIG. 1. Schematic representation of three diagnostics used in measurements of plasma rotation in PDX: Fast Rotating Mirror (FARM) system (top figure), Bragg X-ray crystal spectrometer (middle figure), and Mirnov coil array (bottom).

FIG. 2. Overlay of two spectral scans of Ti XVII from same discharge 10 msec apart and approximately 250 msec after neutral injection. Chordal line of sight was parallel to plasma current.

FIG. 3. Poloidal rotation of C V in neutral beam heated circular discharge. Positive velocity represents ion diamagnetic direction.

FIG. 4. Poloidal rotation of Ti XVII. Each triangle represents an average of five to ten individual Doppler measurements. For these discharges P_{inj}= 3.0 MW $D^0 \rightarrow H^+$, $I_p = 400$ kA, $\overline{n_e} = 2.9 \times 10^{13}\text{cm}^{-3}$.

FIG. 5. Central toroidal velocity for $D^0 \rightarrow H^+$ circular discharges vs. $P_{abs}/\overline{n_e}$. The triangles correspond to I_p = 200-300 kA, the open circles, 300-400 kA, and the dark circles, 400-500 kA.

FIG. 6. Central toroidal velocity for $H^0 \rightarrow D^+$ diverted discharges and $D^0 \rightarrow D^+$ circular discharges vs. $P_{abs}/\overline{n_e}$. The circles represent diverted plasmas with hydrogen injection, and the triangle, a circular discharge with deuterium injection.

FIG. 7. Time evolution of toroidal rotation at r=0 and r=25 cm.

FIG. 8. Decay time of central toroidal rotation vs. $\overline{n_e}$ (*a*) and I_p (*b*).

FIG. 9. Radial profiles of toroidal rotation in two beam heated discharges. For (*a*) parameters are identical with those in Fig. 8; for (*b*) B_T=15 kG, P_{abs}= 2.6 MW $D^0 \rightarrow H^+$, $I_p = 370$ kA, $\overline{n_e} = 4.8 \times 10^{13}\text{cm}^{-3}$.

FIG. 10. Toroidal rotation profile in neutral beam heated circular discharges normalized by $P_{abs}/\overline{n_e}$. Solid and open circles denote co- and counter injection, respectively. Solid line represents normalized toroidal rotation

profile in Fig. 8 (a).

FIG. 11. Toroidal rotation of C V on inner and outer major radius side of plasma. Positive velocity corresponds to direction parallel to current.

FIG. 12. Viscosity profiles which give best fit to the data presented in Figs. 8 (a) and (b) for different values of τ_{CX}. Curve A assumes standard neutral density and temperature profile, in curve B $n_0 \rightarrow 3n_0$, and in curve C, $T_0 \rightarrow 0$.

PDX PLASMA ROTATION

I Fast Rotating Mirror System - Poloidal and Toroidal Rotation Profiles (Doppler Shift ; 2000-6000 Å)

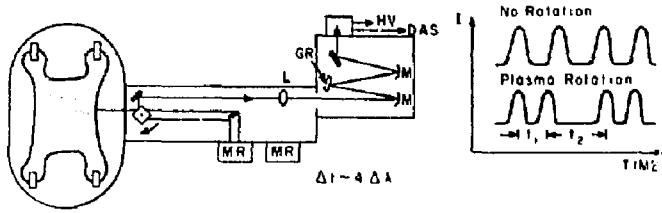

II High Resolution Crystal Spectrometer - Central Toroidal Rotation (Doppler Shift of Ti XXI 261 Å)

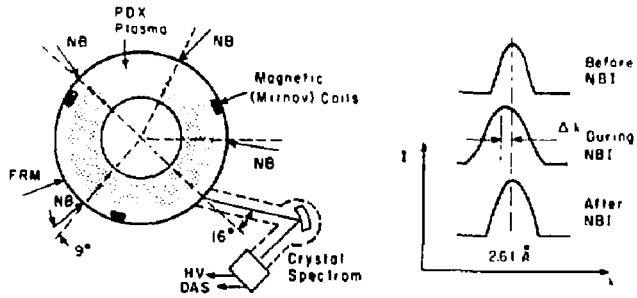

III Magnetic Coils - Poloidal + Toroidal Rotation (Waves Shift).

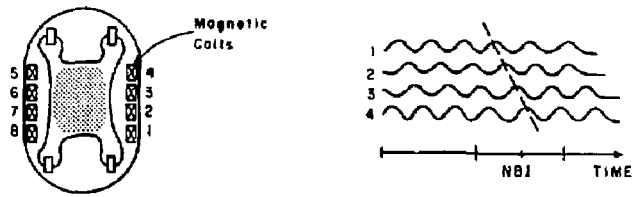

Fig. 1

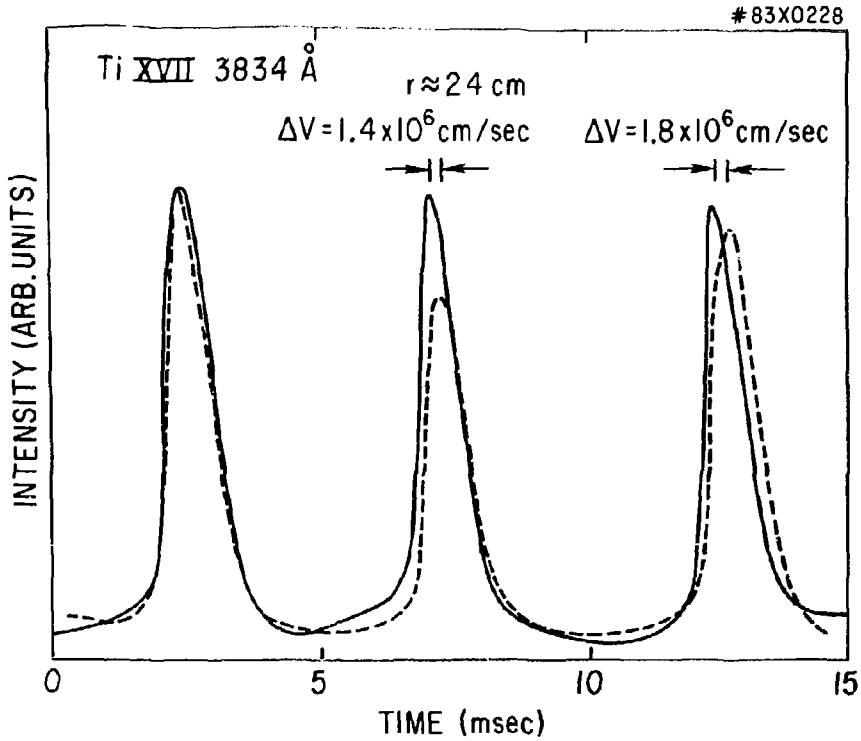
#83X0228
Ti XVII 3834 Å
r≈24 cm
ΔV=1.4x10^6cm/sec
ΔV=1.8x10^6cm/sec
INTENSITY (ARB.UNITS)
0
5
10
15
TIME (msec)

Fig. 2

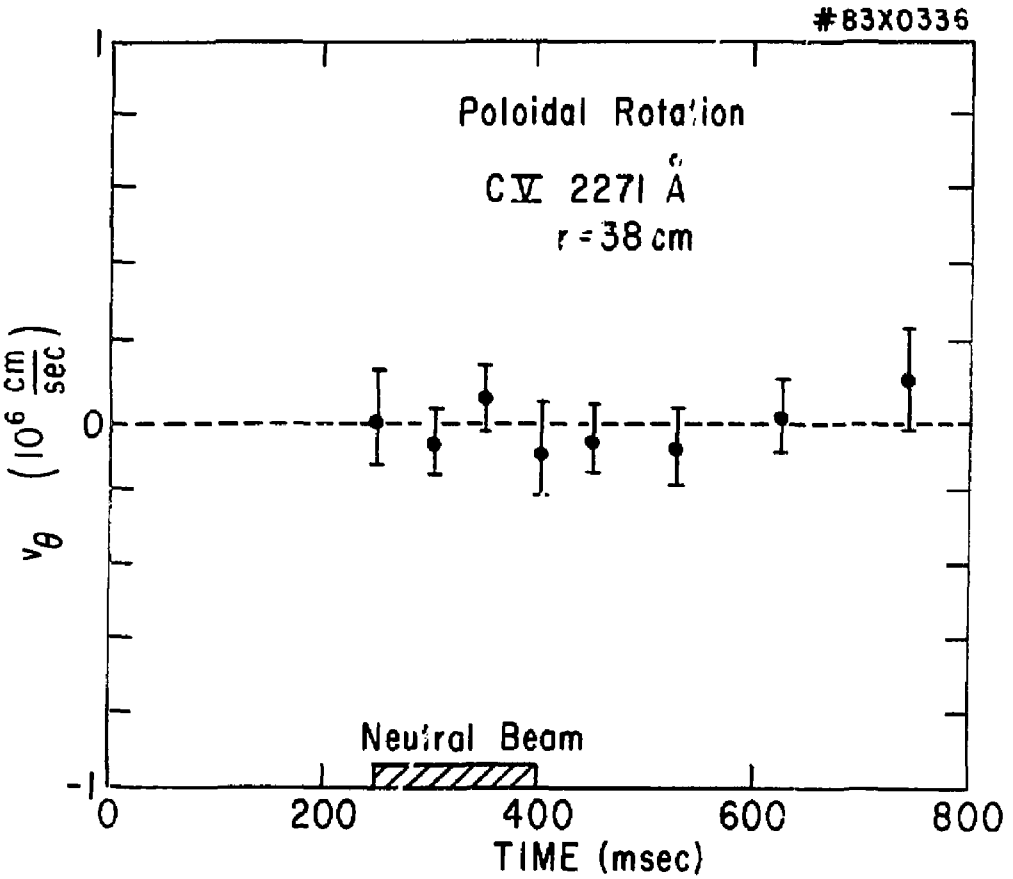
#83X0336
Poloidal Rotation
CVI 2271 Å
r = 38 cm
v_θ ($10^6 \frac{cm}{sec}$)
1
0
-1
Neutral Beam
0
200
400
600
800
TIME (msec)

Fig. 3

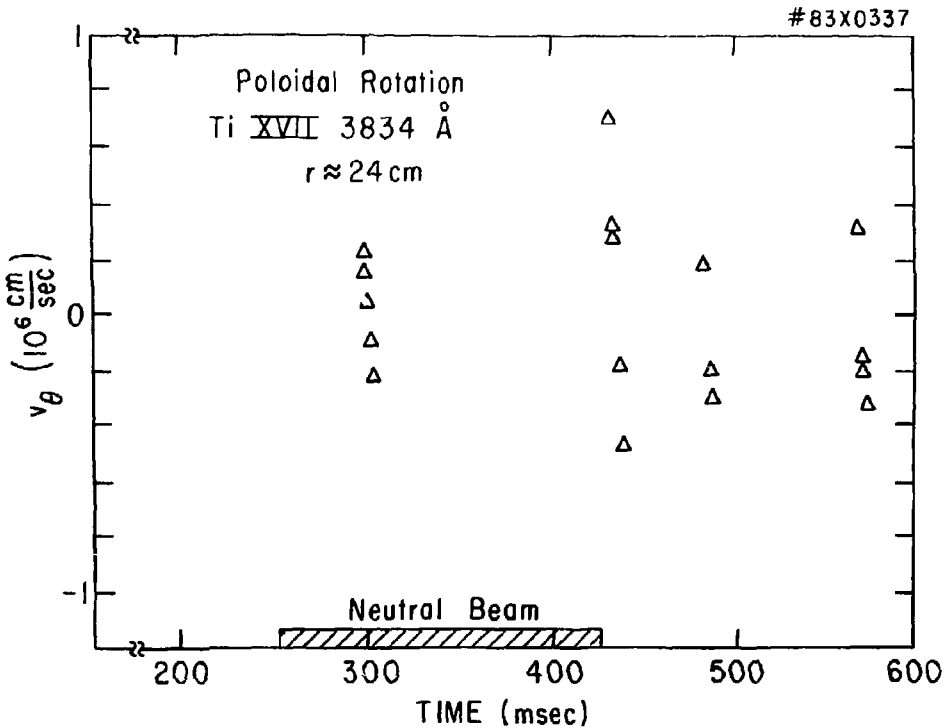
#83X0337
Poloidal Rotation
Ti XVII 3834 Å
r ≈ 24 cm
v_θ ($10^6 \frac{cm}{sec}$)
1
0
-1
Neutral Beam
200
300
400
500
600
TIME (msec)

Fig. 4

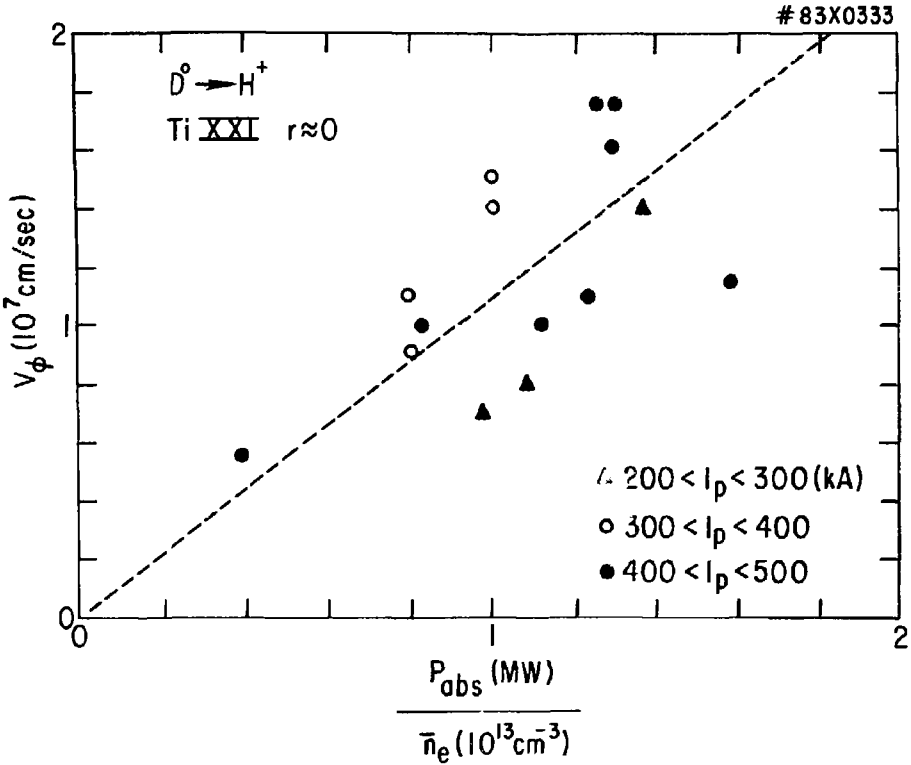
#83X0333
$D^0 \rightarrow H^+$
Ti XXI r≈0
V_ϕ (10^7 cm/sec)
$\frac{P_{abs}\,(MW)}{\bar{n}_e\,(10^{13}cm^{-3})}$
200 < I_p < 300 (kA)
300 < I_p < 400
400 < I_p < 500
0
1
2

Fig. 5

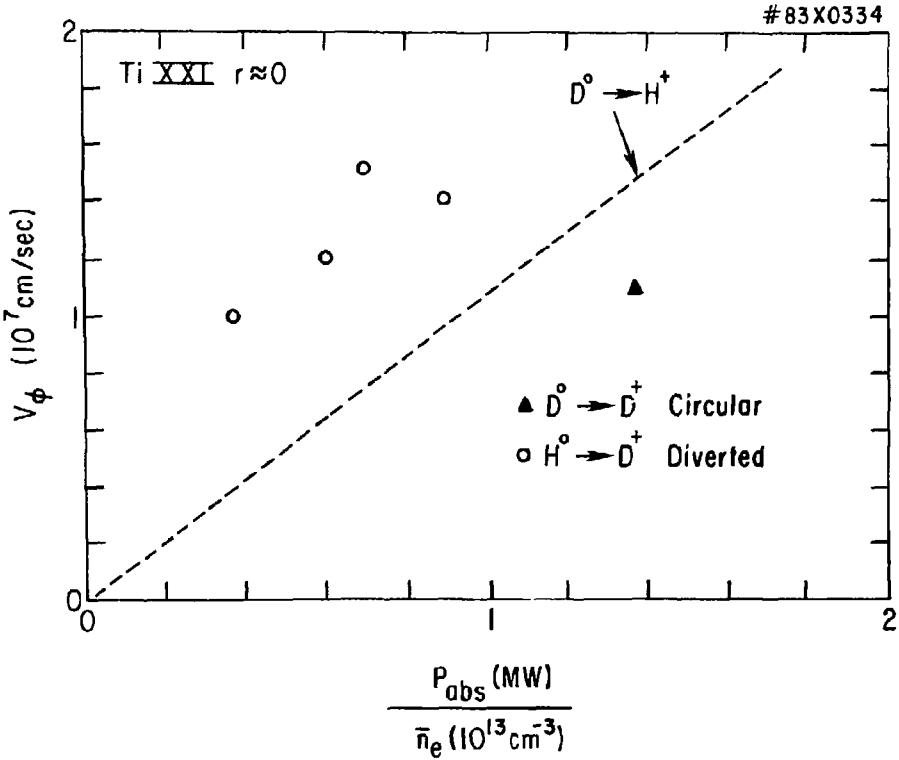
#83X0334
Ti XXI r≈0
D° → H⁺
▲ D° → D⁺ Circular
o H° → D⁺ Diverted
V_ϕ (10^7cm/sec)
$\frac{P_{abs}\,(MW)}{\bar{n}_e\,(10^{13}cm^{-3})}$
0
1
2

Fig. 6

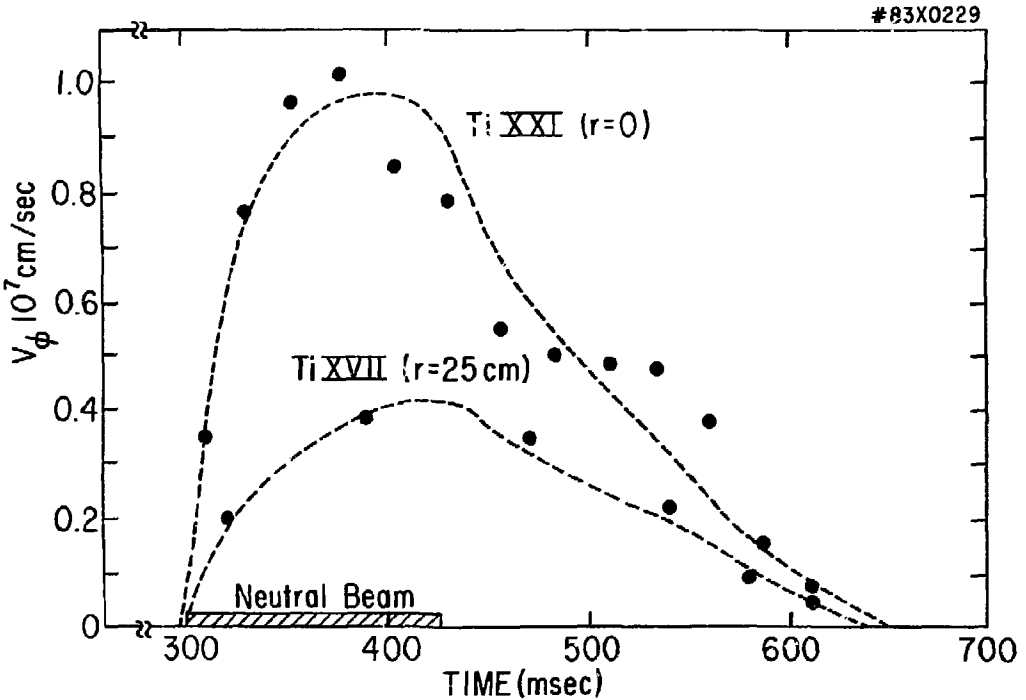
#83X0229
1.0
0.8
0.6
0.4
0.2
0
V_ϕ 10^7cm/sec
Ti XXI (r=0)
Ti XVII (r=25 cm)
Neutral Beam
300
400
500
600
700
TIME (msec)

Fig. 7

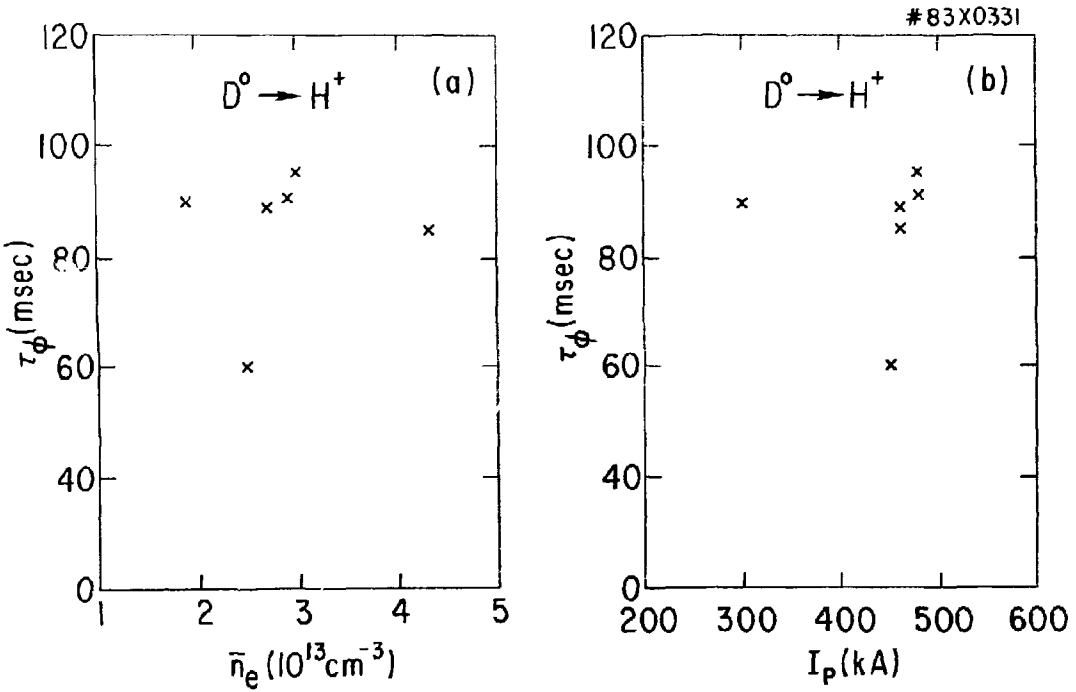
#83X0331
120
100
80
60
40
0
τ_ϕ(msec)
$D^0 \rightarrow H^+$
(a)
1
2
3
4
5
$\bar{n}_e (10^{13} cm^{-3})$
(b)
200
300
400
500
600
I_P(kA)

Fig. 8

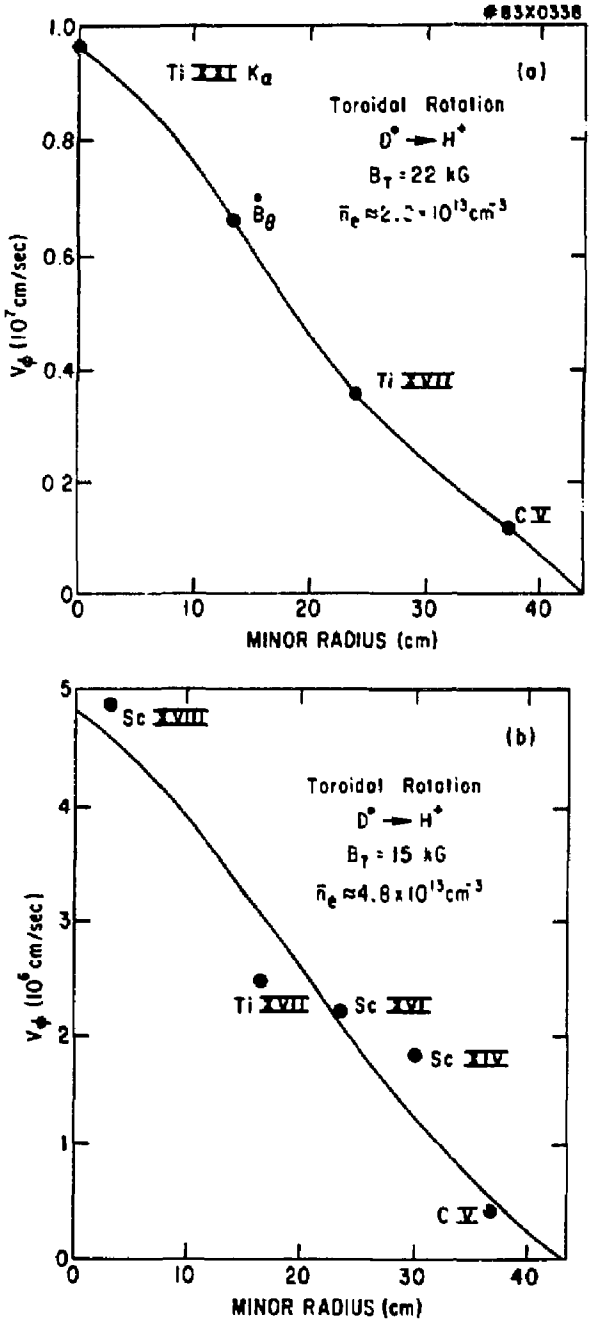
#83X0338
Ti XXII Kα
(a)
Toroidal Rotation
D° → H⁺
B_T = 22 kG
n̄_e ≈ 2.5 × 10^13 cm^-3
B_θ
Ti XVII
C V
V_φ (10^7 cm/sec)
MINOR RADIUS (cm)
Sc XVIII
(b)
Toroidal Rotation
D° → H⁺
B_T = 15 kG
n̄_e ≈ 4.8 × 10^13 cm^-3
Ti XVII
Sc XVI
Sc XIV
C V
V_φ (10^6 cm/sec)
MINOR RADIUS (cm)

Fig. 9

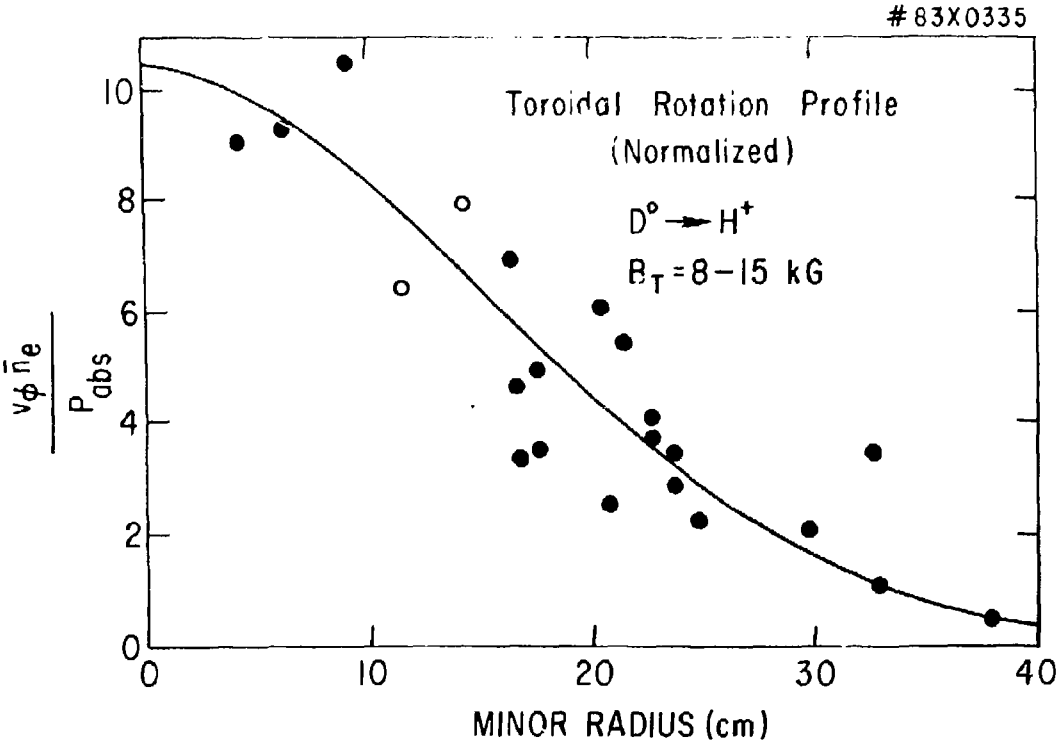
#83X0335
Toroidal Rotation Profile
(Normalized)
D° → H⁺
B_T = 8–15 kG
v_φ n̄_e / P_abs
MINOR RADIUS (cm)
0
2
4
6
8
10
0
10
20
30
40

Fig. 10

#83X0332

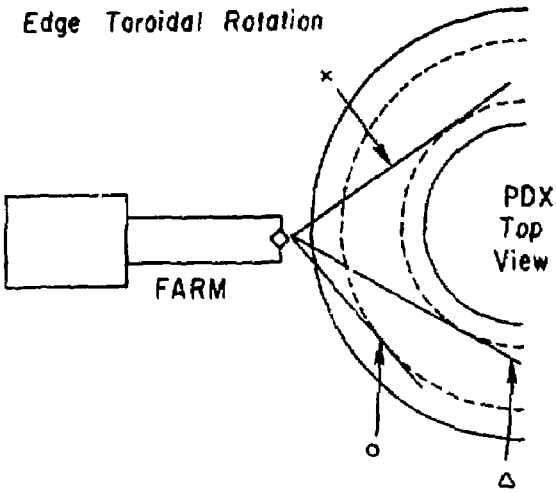

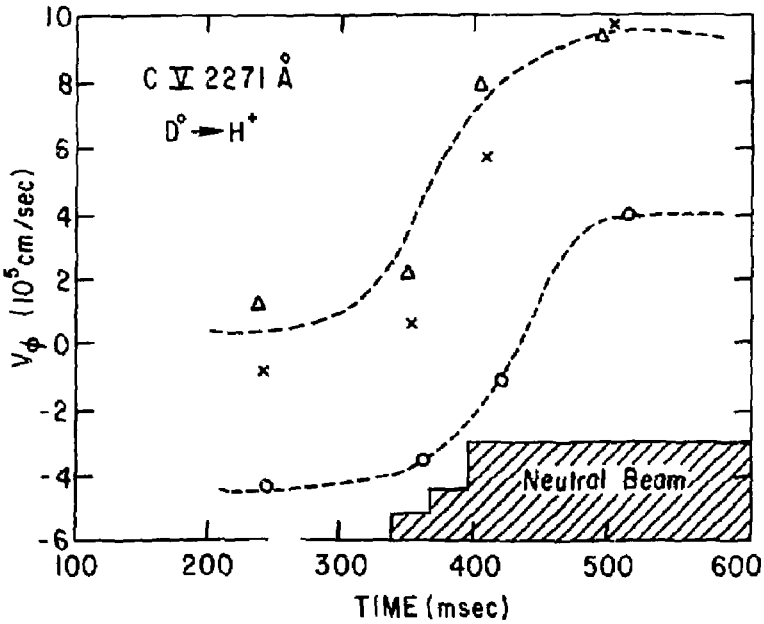

Fig. 11

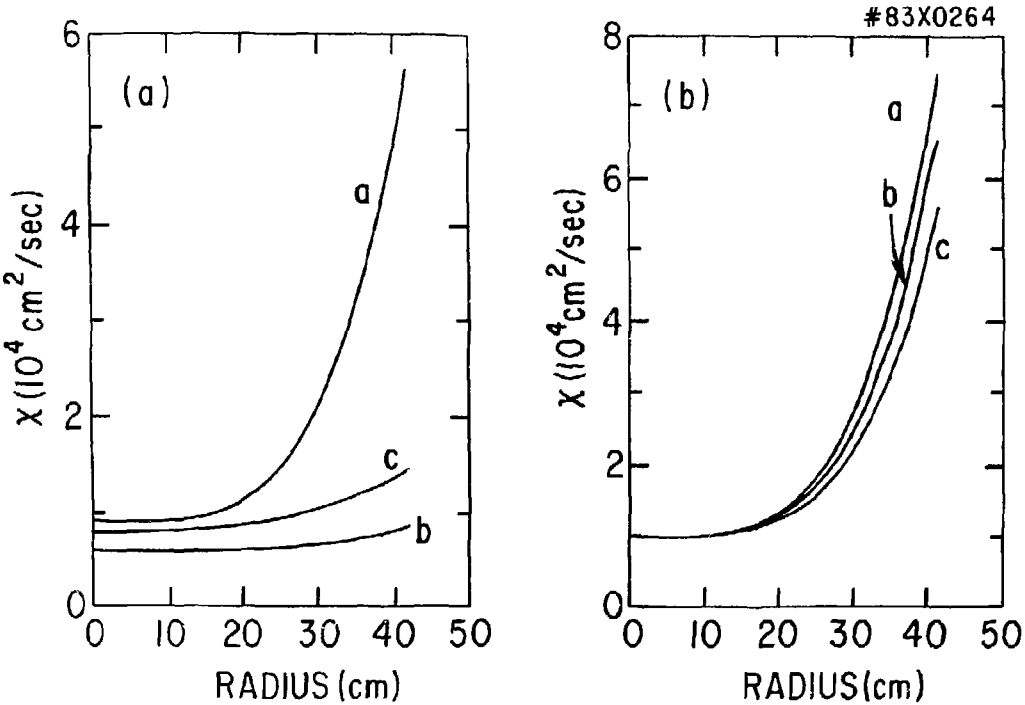

Fig. 12

EXTERNAL DISTRIBUTION IN ADDITION TO TIC UC-20

Plasma Res Lab, Austra Nat'l Univ, AUSTRALIA
Dr. Frank J. Paoloni, Univ of Wollongong, AUSTRALIA
Prof. I.R. Jones, Flinders Univ., AUSTRALIA
Prof. M.H. Brennan, Univ Sydney, AUSTRALIA
Prof. F. Cap, Inst Theo Phys, AUSTRIA
Prof. Frank Verheest, Inst theoretische, BELGIUM
Dr. D. Palumbo, Dg XII Fusion Prog, BELGIUM
Ecole Royale Militaire, Lab de Phys Plasmas, BELGIUM
Dr. R.H. Sakanaka, Univ Estadual, BRAZIL
Dr. C.R. Jones, Univ of Alberta, CANADA
Prof. J. Teichmann, Univ of Montreal, CANADA
Dr. M.W. Skerscerd, Univ of Saskatchewan, CANADA
Prof. S.R. Sreenivasan, University of Calgary, CANADA
Prof. Tudor W. Johnston, INRS-Energie, CANADA
Dr. Hannes Barnard, Univ British Columbia, CANADA
Dr. R.P. Bachynski, MPB Technologies, Inc., CANADA
Zhengxu Li, SW Inst Physics, CHINA
Library, Tsing Hua University, CHINA
Librarian, Institute of Physics, CHINA
Inst Plasma Phys, SW Inst Physics, CHINA
Dr. Peter Lukac, Komenskeho Univ, CZECHOSLOVAKIA
The Librarian, Culham Laboratory, ENGLAND
Prof. Schatzman, Observatoire de Nice, FRANCE
J. Radet, CEN-BP6, FRANCE
AM Dupas Library, AM Dupas Library, FRANCE
Dr. Tom Muni, Academy Bibliographic, HONG KONG
Preprint Library, Cent Res Inst Phys, HUNGARY
Dr. A.K. Sundaram, Physical Research Lab, INDIA
Dr. S.K. Trehan, Panjab University, INDIA
Dr. Indra, Mohan Lal Das, Benaras Hindu Univ, INDIA
Dr. L.K. Chavda, South Gujarat Univ, INDIA
Dr. R.K. Chhajlani, Var Ruchi Marg, INDIA
P. Kaw, Physical Research Lab, INDIA
Dr. Phillip Rosenau, Israel Inst Tech, ISRAEL
Prof. S. Cuperman, Tel Aviv University, ISRAEL
Prof. G. Rostagni, Univ Di Padova, ITALY
Librarian, Int'l Ctr Theo Phys, ITALY
Miss Clelia De Palo, Assoc EURATOM-CNEN, ITALY
Biblioteca, del CNR EURATOM, ITALY
Dr. K. Yamato, Toshiba Res & Dev, JAPAN
Prof. M. Yoshikawa, JAERI, Tokai Res Est, JAPAN
Prof. T. Uchida, University of Tokyo, JAPAN
Research Info Center, Nagoya University, JAPAN
Prof. Kyoji Nishikawa, Univ of Hiroshima, JAPAN
Prof. Sigeru Mori, JAERI, JAPAN
Library, Kyoto University, JAPAN
Prof. Ichiro Kawakami, Nihon Univ, JAPAN
Prof. Setoshi Itoh, Kyushu University, JAPAN
Tech Info Division, Korea Atomic Energy, KOREA
Dr. R. Englend, Ciudad Universitaria, MEXICO
Bibliotheek, Fom-Inst Voor Plasma, NETHERLANDS
Prof. B.S. Liley, University of Waikato, NEW ZEALAND
Dr. Suresh C. Sharma, Univ of Calabar, NIGERIA
Prof. J.A.C. Cabral, Inst Superior Tech, PORTUGAL
Dr. Octavian Petrus, ALI CUZA University, ROMANIA
Dr. R. Jones, Nat'l Univ Singapore, SINGAPORE
Prof. M.A. Hellberg, University of Natal, SO AFRICA
Dr. Johan de Villiers, Atomic Energy Bd, SO AFRICA
Dr. J.A. Tagle, JEN, SPAIN
Prof. Hans Wilhelmson, Chalmers Univ Tech, SWEDEN
Dr. Lennart Stenflo, University of UMEA, SWEDEN
Library, Royal Inst Tech, SWEDEN
Dr. Erik T. Karlson, Uppsala Universitet, SWEDEN
Centre de Recherchesen, Ecole Polytech Fed, SWITZERLAND
Dr. W.L. Weise, Nat'l Bur Stand, USA
Dr. W.M. Stacey, Georg Inst Tech, USA
Dr. S.T. Wu, Univ Alabama, USA
Prof. Norman L. Oleson, Univ S Florida, USA
Dr. Benjamin Ma, Iowa State Univ, USA
Prof. Magne Kristiansen, Texas Tech Univ, USA
Dr. Raymond Askew, Auburn Univ, USA
Dr. V.T. Tolok, Kharkov Phys Tech Ins, USSR
Dr. D.D. Ryutov, Siberian Acad Sci, USSR
Dr. M.S. Rabinovich, Lebedev Physical Inst, USSR
Dr. G.A. Ellseev, Kurchatov Institute, USSR
Dr. V.A. Glukhikh, Inst Electro-Physical, USSR
Prof. T.J. Boyd, Univ College N Wales, WALES
Dr. K. Schindler, Ruhr Universitat, W. GERMANY
Nuclear Res Estab, Julich Ltd, W. GERMANY
Librarian, Max-Planck Institut, W. GERMANY
Dr. H.J. Kaeppler, University Stuttgart, W. GERMANY
Bibliothek, Inst Plasmaforschung, W. GERMANY